11) Shirato, M., T. Aragaki and E. Iritani: *J. Chem. Eng. Japan*, **13**, 61 (1980).
12) Shirato, M., T. Aragaki, E. Iritani and T. Funahashi: *J. Chem. Eng. Japan*, **13**, 473 (1980).
13) Yoshioka, N., K. Ueda and T. Hirao: *Kagaku Kōgaku*, **33**, 80 (1969).
14) Yoshioka, N., K. Ueda and K. Miyoshi: *J. Chem. Eng. Japan*, **5**, 291 (1972).

(Presented at the 14th Autumn Meeting at Yokohama, October 1980 and at the 15th Autumn Meeting at Kanazawa, October 1981, of The Society of Chemical Engineers, Japan.)

DISSOLUTION OF A BENZOIC ACID WALL INTO AQUEOUS ALKALINE SOLUTIONS FLOWING LAMINARLY IN A PARALLEL-PLATE DUCT

JULIO H. EGOCHEAGA, MASAKO OKUNO, TOSHIKUNI YONEMOTO AND TEIRIKI TADAKI

Department of Chemical Engineering, Tohoku University, Sendai 980

Key Words: Mass Transfer, Dissolution, Simulation, Ionic Migration, Convective Mass Transfer, Parallel-Plate Channel, Solid-Liquid Reaction

Mass transfer accompanied by dissolution of benzoic acid from the wall of a parallel-plate duct into aqueous alkaline solutions was studied, using a theoretical model based on diffusion equations. Chemical and ionic interactions of each species, together with diffusion and convection, are considered in this analysis. The theoretical equations were solved as an initial-value problem by using a finite-difference technique. Simultaneously, experiments were conducted under laminar-flow conditions to check the predicted overall rates of dissolution. The rate of dissolution of benzoic acid into KOH solutions was shown to be faster than that into LiOH solutions of equal concentration because of the larger mobility of the K^+ ions. Under the conditions analyzed here, the agreement between theoretical and experimental overall rates of dissolution was excellent. This showed that the present theoretical analysis can be valid and useful in predicting rates of mass transfer in this kind of complex solid-liquid dissolution systems.

Introduction

Simultaneous diffusion, convection, chemical reactions and ionic migration are often involved in solid-liquid mass transfer. The theory is well established for simple flow and reaction systems where mass transfer occurs mainly due to the first three mechanisms.[1,3,5] However, few theoretical analyses seem to be available for the more complex but still common case where effects of partial dissociation of dissolving species and of ionic migration cannot be neglected.

In the present paper a theoretical model based on diffusion equations is used to analyze the dissolution of benzoic acid from the wall of a parallel-plate duct into a laminar stream of aqueous KOH or LiOH solutions flowing inside the duct. This system was selected because its transport characteristics are strongly influenced by the chemical equilibria between the dissolved species and by liquid-phase ionic migration, and because its hydrodynamic and physical properties are well enough known to permit experimental verification of the theoretical analysis.[10,14]

A finite-difference method with overrelaxation technique was used to solve the proposed model. The validities of the mathematical formulation and the method of solution were checked by comparing theoretical and experimental overall rates of dissolution. Finally, the influences of flow rate, alkali concentration and type of alkali cation on the dissolution process are discussed on the basis of overall rates of dissolution and concentration profiles obtained from the present analysis.

1. Theory

1.1 Model formulation

Consider the dissolution of benzoic acid from the lower wall of a parallel-plate duct into a laminar stream of aqueous KOH or LiOH flowing inside the

Received August 31, 1984. Correspondence concerning this article should be addressed to T. Tadaki.

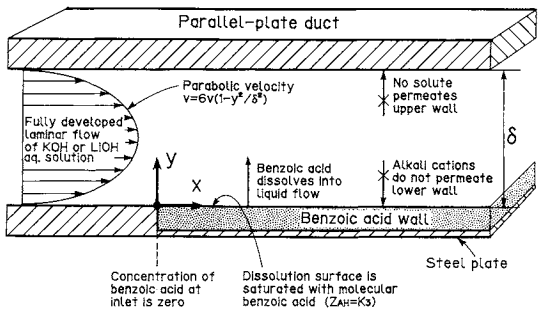

Fig. 1. Schematic representation of two-dimensional dissolution process in a parallel-plate duct.

duct, as shown in **Fig. 1**. Benzoic acid dissolves at the solid-liquid interface according to the following reversible process:

$$AH_{(s)} \rightleftharpoons AH_{(aq)} \tag{1}$$

Simultaneously, two reversible reactions take place in the liquid phase:

$$AH_{(aq)} \rightleftharpoons A^-_{(aq)} + H^+_{(aq)} \tag{2}$$

$$H^+_{(aq)} + OH^-_{(aq)} \rightleftharpoons H_2O \tag{3}$$

Both reactions are instantaneous and reversible.[2,4]

Mass transfer in this system is now modeled by assuming local equilibrium, a dilute and isothermal solution, constant physical properties, instantaneous saturation at the dissolution surface with molecular benzoic acid, fully developed laminar flow, negligible diffusion and migration in the flow direction, negligible changes in the geometry of the benzoic acid surface and steady state.

Then, using δ, C_T^* and $6\bar{v}$, respectively, as the characteristic length, concentration and velocity, the flux and diffusion equations for each species can be written in dimensionless form as[9]

$$\vec{\mathcal{N}}_i = -\left(S_i \frac{\partial Z_i}{\partial Y} + n_i S_i Z_i \frac{\partial \Phi}{\partial Y}\right)\vec{j} + V Z_i \vec{i}, \qquad i=1\text{–}5 \tag{4}$$

$$S_i \frac{\partial^2 Z_i}{\partial Y^2} + n_i S_i \frac{\partial}{\partial Y}\left(Z_i \frac{\partial \Phi}{\partial Y}\right) - V\frac{\partial Z_i}{\partial X} + \mathcal{R}_i = 0, \qquad i=1\text{–}5 \tag{5}$$

where $1=AH$, $2=A^-$, $3=OH^-$, $4=H^+$ and $5=M^+$. Here, the stoichiometric relations are

$$\mathcal{R}_{AH} + \mathcal{R}_A = 0 \tag{6}$$

$$\mathcal{R}_M = 0 \tag{7}$$

Thus, combining Eqs. (5) with (6) and (7) we obtain

$$S_{AH}\frac{\partial^2 Z_{AH}}{\partial Y^2} + S_A \frac{\partial^2 Z_A}{\partial Y^2} - S_A \frac{\partial}{\partial Y}\left(Z_A \frac{\partial \Phi}{\partial Y}\right) - V\frac{\partial}{\partial X}(Z_{AH} + Z_A) = 0 \tag{8}$$

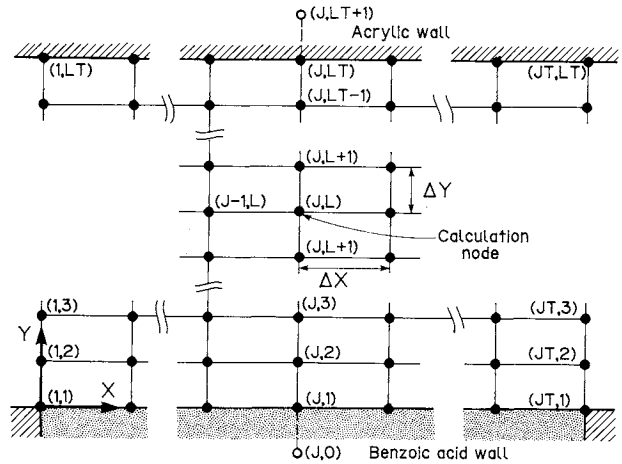

Fig. 2. Finite-difference grid system.

$$S_M \frac{\partial^2 Z_M}{\partial Y^2} + S_M \frac{\partial}{\partial Y}\left(Z_M \frac{\partial \Phi}{\partial Y}\right) - V\frac{\partial Z_M}{\partial X} = 0 \tag{9}$$

The system is electrically neutral and no electric current exists, so we can write

$$\sum_{i=2}^{5} n_i Z_i = 0 \tag{10}$$

$$\sum_{i=2}^{5} n_i \vec{\mathcal{N}}_i = 0 \tag{11}$$

Further, the chemical equilibrium relations of reactions (2) and (3) are

$$K_1 = Z_A \cdot Z_H / Z_{AH} \tag{12}$$

$$K_2 = Z_H \cdot Z_{OH} \tag{13}$$

Thus, Eqs. (10), (12) and (13) can be manipulated to yield

$$Z_H = 0.5[\{Z_M + 4(K_1 \cdot Z_{AH} + K_2)\}^{1/2} - Z_M] \tag{14}$$

and an explicit expression for the electrostatic potential can be derived from Eqs. (4), (10) and (11)[15]:

$$\frac{\partial \Phi}{\partial Y} = -\left(\sum_{i=2}^{5} n_i S_i \frac{\partial Z_i}{\partial Y}\right) \Big/ \left(\sum_{i=2}^{5} n_i^2 S_i Z_i\right) \tag{15}$$

As for the boundary conditions, at $Y=0$ the surface is saturated with molecular benzoic acid and normal flux of M^+ is zero:

$$Y=0, \qquad Z_{AH} = K_3 \tag{16}$$

$$\frac{\partial Z_M}{\partial Y} + Z_M \frac{\partial \Phi}{\partial Y} = 0 \tag{17}$$

At $Y=1$ all normal fluxes vanish and the following equations apply[11]:

$$Y=1, \qquad \frac{\partial Z_i}{\partial Y} = 0 \qquad i=1\text{–}5 \tag{18}$$

$$\frac{\partial \Phi}{\partial Y} = 0 \tag{19}$$

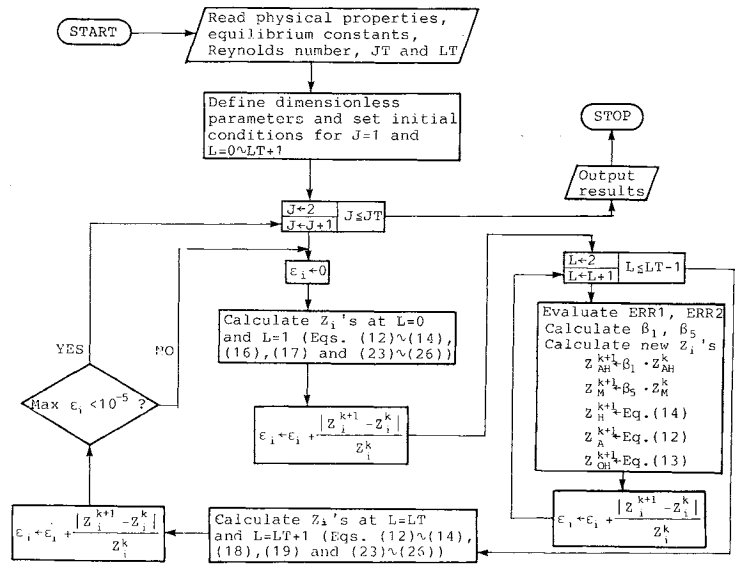

Fig. 3. Flow chart for calculation of dissolution process.

Finally, conditions at the inlet are

$$X=0\,, \qquad Z_{AH}=0 \tag{20}$$

$$Z_A=0 \tag{21}$$

$$Z_M=Z_{M_0} \tag{22}$$

1.2 Numerical calculation

Equations (8), (9) and (15) were treated as an initial-value problem and written in finite-difference form by using backward-difference approximations for $\partial/\partial X$ and central-difference approximations for $\partial/\partial Y$ and $\partial^2/\partial Y^2$. The grid system used to set up the formulation is shown in **Fig. 2**. For a given node, (J, L) the results are

$$\frac{S_{AH}}{(\Delta Y)^2}\{Z_{AH_{J,L+1}}-2Z_{AH_{J,L}}+Z_{AH_{J,L-1}}\}$$
$$+\frac{S_A}{(\Delta Y)^2}\{Z_{A_{J,L+1}}-2Z_{A_{J,L}}+Z_{A_{J,L-1}}\}$$
$$-\frac{S_A}{\Delta Y}\left\{\frac{Z_{A_{J,L+1}}+Z_{A_{J,L}}}{2}P_{J,L}-\frac{Z_{A_{J,L}}+Z_{A_{J,L-1}}}{2}Q_{J,L}\right\}$$
$$-\frac{V}{\Delta X}\{(Z_{AH_{J,L}}+Z_{A_{J,L}})-(Z_{AH_{J-1,L}}+Z_{A_{J-1,L}})\}=0 \tag{23}$$

$$\frac{S_M}{(\Delta Y)^2}\{Z_{M_{J,L+1}}-2Z_{M_{J,L}}+Z_{M_{J,L-1}}\}$$
$$+\frac{S_M}{\Delta Y}\left\{\frac{Z_{M_{J,L+1}}+Z_{M_{J,L}}}{2}P_{J,L}-\frac{Z_{M_{J,L}}+Z_{M_{J,L-1}}}{2}Q_{J,L}\right\}$$
$$-\frac{V}{\Delta X}\{(Z_{M_{J,L}}-Z_{M_{J-1,L}})\}=0 \tag{24}$$

where

$$P_{J,L}=$$
$$-\sum_{i=2}^{5}n_i\frac{S_i}{\Delta Y}(Z_{i_{J,L+1}}-Z_{i_{J,L}})\Big/\sum_{i=2}^{5}n_i^2S_i\left(\frac{Z_{i_{J,L+1}}+Z_{i_{J,L}}}{2}\right) \tag{25}$$

$$Q_{J,L}=$$
$$-\sum_{i=2}^{5}n_i\frac{S_i}{\Delta Y}(Z_{i_{J,L}}-Z_{i_{J,L-1}})\Big/\sum_{i=2}^{5}n_i^2S_i\left(\frac{Z_{i_{J,L}}+Z_{i_{J,L-1}}}{2}\right) \tag{26}$$

Equations (23) to (26) were solved by the iterative procedure outlined in **Fig. 3** under restrictions (12) to (14) and initial and boundary conditions (16) to (22). The required overrelaxation factors β_1 and β_5 are calculated by the method described in the **Appendix**. The algorithm of Fig. 3 showed good numerical stability due to the choice of backward-difference approximations for $\partial/\partial X$ (i.e. the implicit method[8]).

2. Experiment

2.1 Apparatus and method

Figure 4 shows details of the rectangular duct used for the present work. The duct's aspect (2 mm in height, 40 mm in width) was selected so as to reduce side-wall effects and to obtain an almost two-dimensional flow pattern within it. The 50 mm-long benzoic acid wall was prepared by pouring molten benzoic acid in a 2 mm-deep cavity and carefully polishing the solidified acid until a smooth, plain surface was obtained. A duct length of 105 mm, followed by a zone packed with 2-mm glass beads, was provided at both ends of the benzoic acid wall to eliminate inlet and outlet turbulence effects and ensure a completely developed laminar flow profile in the test zone.

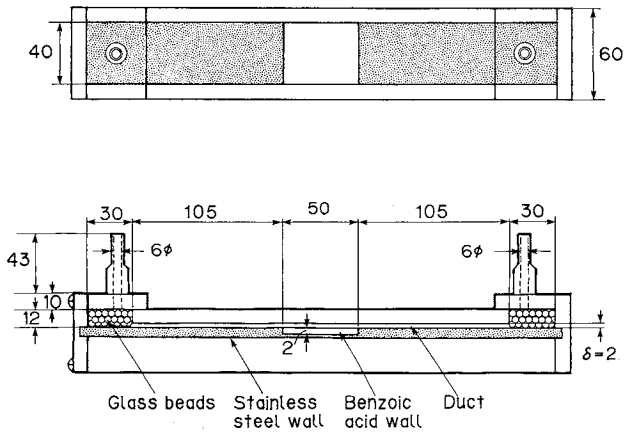

Fig. 4. Schematic diagram of experimental apparatus.

Experiments were conducted at 293 ± 0.5 K using aqueous solutions of KOH or LiOH as liquid phase. These solutions were prepared from primary-grade reagents and standardized with $10\,\mathrm{mol \cdot m^{-3}}$ HCl. Overall rates of dissolution of benzoic acid were calculated from the concentration of total benzoic acid (molecular + anionic) in the effluent liquid, which was measured with a UV spectrophotometer.

Experimental conditions were selected so as to minimize the effects of natural convection while maintaining a low rate of recession of the benzoic acid surface.* These conditions were $Re = 50$–150 and $C_{M_0} = 0$–$30\,\mathrm{mol \cdot m^{-3}}$.

Results were represented as non-dimensional rates of dissolution defined as follows:

$$\mathscr{M} = (\delta/l) \cdot Sc \cdot Re \cdot \bar{Z}_{T_{out}} \tag{27}$$

2.2 Physical properties at 293 K

All properties are listed in **Table 1**. The diffusion coefficient of molecular benzoic acid was taken equal to the overall diffusion coefficient of benzoic acid as defined and measured by Vanadurongwan *et al.*[17] All other properties were obtained from the literature,[6,7,12,13,16] except for K_S, which was calculated from the values of C_T^*, K_{AH}, K_W and the electroneutrality condition.

3. Results and Discussion

The effect of mesh size on computation accuracy was first investigated. For this, the theoretical rates of dissolution corresponding to $Re = 100$ and $C_{M_0} = 10\,\mathrm{mol \cdot m^{-3}}$ were calculated using different mesh sizes. The integral normal flux of total benzoic acid along the dissolution surface and the mixing cap concentration of total benzoic acid in the liquid phase at the end of the soluble wall were computed using Eqs. (28) and (29), respectively.

* The maximum rate of recession of the benzoic acid surface was estimated as 6×10^{-3} mm/min, which represents a maximum change of 5% in the duct's height after a typical run.

Table 1. Physical properties at 293 K

C_T^*	23.75	$[\mathrm{mol \cdot m^{-3}}]$[12]
D_A	7.328×10^{-10}	$[\mathrm{m^2 \cdot s^{-1}}]$[13]
D_{AH}	8.248×10^{-10}	$[\mathrm{m^2 \cdot s^{-1}}]$[17]
D_H	8.506×10^{-9}	$[\mathrm{m^2 \cdot s^{-1}}]$[13]
D_K	1.740×10^{-9}	$[\mathrm{m^2 \cdot s^{-1}}]$[13]
D_{Li}	9.030×10^{-10}	$[\mathrm{m^2 \cdot s^{-1}}]$[13]
D_{OH}	4.685×10^{-9}	$[\mathrm{m^2 \cdot s^{-1}}]$[13]
K_{AH}	6.160×10^{-2}	$[\mathrm{mol \cdot m^{-3}}]$[7]
K_S	22.57	$[\mathrm{mol \cdot m^{-3}}]$
K_W	6.918×10^{-9}	$[\mathrm{mol^2 \cdot m^{-6}}]$[6]
γ	1.007×10^{-6}	$[\mathrm{m^2 \cdot s^{-1}}]$[16]

Table 2. Mass balance and CPU time of numerical calculation
($Re = 100$, $C_{M_0} = 10\,\mathrm{mol \cdot m^{-3}}$, $l = 50$ mm)

Mesh size	$6\mathscr{F}$ [—]	$\bar{Z}_{T\,out}$ [—]	CPU time [s]
100×51 $\left(\begin{matrix}\Delta X = 0.25 \\ \Delta Y = 0.02\end{matrix}\right)$	8.58×10^{-3}	8.54×10^{-3}	7.67
100×101 $\left(\begin{matrix}\Delta X = 0.25 \\ \Delta Y = 0.01\end{matrix}\right)$	8.70×10^{-3}	8.71×10^{-3}	25.12
100×201 $\left(\begin{matrix}\Delta X = 0.25 \\ \Delta Y = 0.005\end{matrix}\right)$	8.76×10^{-3}	8.76×10^{-3}	168.28
250×201 $\left(\begin{matrix}\Delta X = 0.1 \\ \Delta Y = 0.005\end{matrix}\right)$	8.76×10^{-3}	8.76×10^{-3}	197.98

$$\mathscr{F} = -\int_0^{l/\delta} \left(S_{AH} \frac{\partial Z_{AH}}{\partial Y} + S_A \frac{\partial Z_A}{\partial Y} - S_A Z_A \frac{\partial \Phi}{\partial Y} \right)\Bigg|_{Y=0} dX \tag{28}$$

$$\bar{Z}_{T_{out}} = 6 \int_0^1 V(Z_{AH} + Z_A)\Big|_{x=l/\delta} dY \tag{29}$$

where l/δ is taken as 25. Overall mass balance requires that

$$\bar{Z}_{T_{out}} = 6\mathscr{F} \tag{30}$$

Table 2 shows that Eq. (30) is satisfied with increasing accuracy as ΔY is reduced. It further shows that mesh sizes of $\Delta X = 0.1$ and $\Delta Y = 0.005$ suffice to obtain accurate results in a reasonable CPU time. Accordingly, subsequent calculations were performed only with these mesh sizes.

Theoretical overall rates of dissolution are shown together with the experimental data in **Fig. 5**. Within the experimental conditions, an almost quantitative agreement exists between theory and experiment, showing that the assumptions made in the present model were pertinent and that the calculation procedure was efficient. The figure also indicates that dissolution rates are faster in the presence of K^+ as compared with Li^+. The difference in rate of disso-

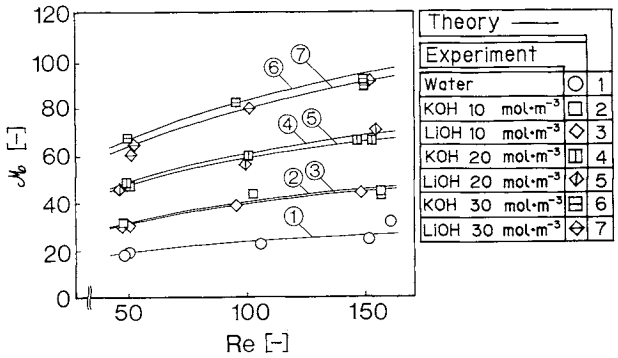

Fig. 5. Comparison of theoretical and experimental results (effect of alkali cation).

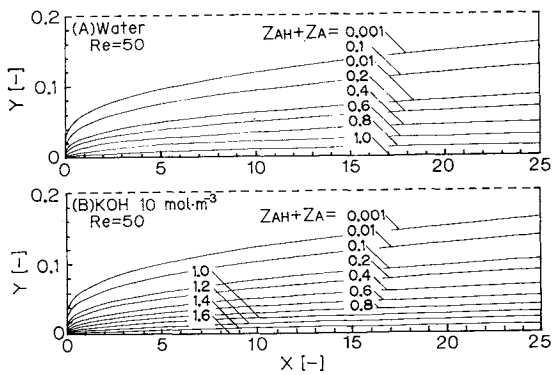

Fig. 6. Theoretical concentration contours of total benzoic acid within testing zone at $Re=50$. (A) dissolution in water; (B) dissolution in KOH 10 mol·m^{-3}.

lution becomes larger as the initial concentration of alkali is increased.

The increase in rate of dissolution due to the presence of alkali is explained in **Fig. 6**, which shows the theoretical concentration contours of total benzoic acid at $Re=50$ for dissolution in water and in 10 mol·m^{-3} KOH solution. This figure indicates that both the surface concentration and the concentration gradient of total benzoic acid are larger in the KOH solution. The main cause of this difference is that the equilibria of reactions (2) and (3) lie more to the right in the presence of alkali. In both cases, (A) and (B), the concentration of molecular benzoic acid at $Y=0$ is fixed according to Eq. (16). However, the concentration of anionic benzoic acid changes in the presence of alkali, and its value is established so as to satisfy boundary condition (17) and equilibrium relations (12) and (13). These results are not in conflict with the general assumption that the concentration of dissolving species is constant at the interface, because the dissolving species is only the molecular form of the acid.

The effect of alkali cation type is explained in **Fig. 7**, which shows the theoretical concentration distribution of alkali cation, (A), and total benzoic acid,

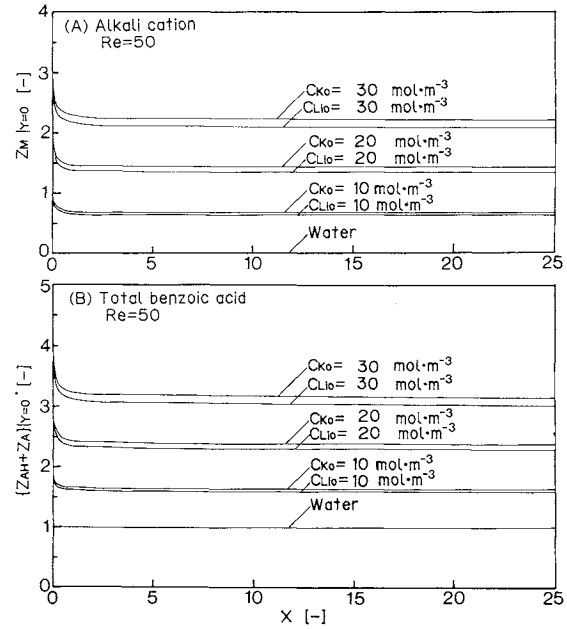

Fig. 7. Theoretical concentration profiles of alkali cation (A) and total benzoic acid (B) along X at $Y=0$ for $Re=50$ and $C_{M_0}=0$–30 mol·m^{-3}.

(B), at $Y=0$ along X for different concentrations of KOH and LiOH. It can be seen that for an identical alkali concentration at the inlet, Z_K is larger than Z_{Li}. As predicted by Eqs. (12) and (14), this causes Z_A (and therefore $Z_{AH}+Z_A$) to be higher when the alkali cation is K^+, as figure (B) shows. This difference in total benzoic acid concentration at $Y=0$ partly explains why rates of dissolution are faster in the presence of K^+ as compared with Li^+.

To further analyze the dissolution process, the theoretical concentration profiles along Y for $Re=50$ and $X=12.5$ are shown in **Fig. 8**. Figure (A) corresponds to water and 10 mol·m^{-3} KOH solution, while figure (B) corresponds to 30 mol·m^{-3} solutions of KOH and LiOH. These figures show that a reaction plane between AH and OH^- is formed near the interface when alkali is present. The distance from the interface to this plane becomes smaller as C_{M_0} is increased. The diffusion of OH^- ions from the bulk of the liquid towards the reaction plane implies the simultaneous transport of their counterions, the M^+ ions (this is migrative transfer). As the magnitude of this transport partly depends on the mobility of the alkali cation itself, KOH is transported faster than LiOH (see Table 1), and the reaction plane is formed closer to the interface in the former case. The result is a larger concentration gradient of AH between the reaction plane and $Y=0$, that is, a larger rate of dissolution in the presence of K^+. This explains the observed differences between rates of dissolution in KOH and LiOH solutions.

Finally, **Fig. 9** shows the profiles at $X=2.5$, under

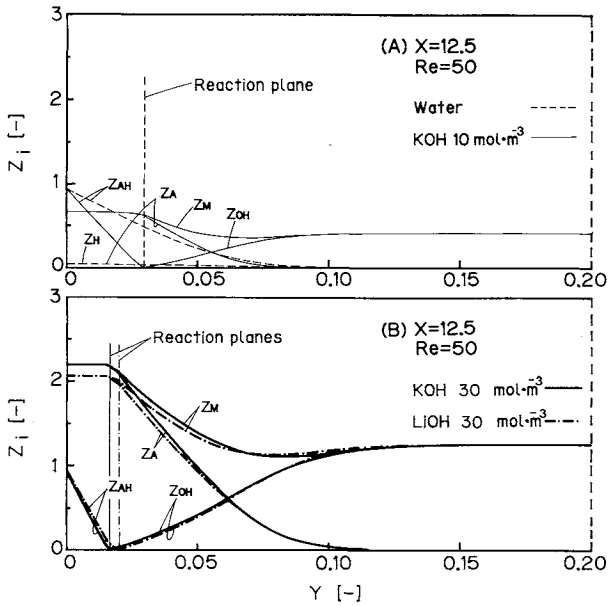

Fig. 8. Theoretical distribution of individual species along the Y direction at $X=12.5$. (A) dissolution into water and 10 mol·m^{-3} KOH solution; (B) dissolution into 30 mol·m^{-3} KOH and LiOH solutions.

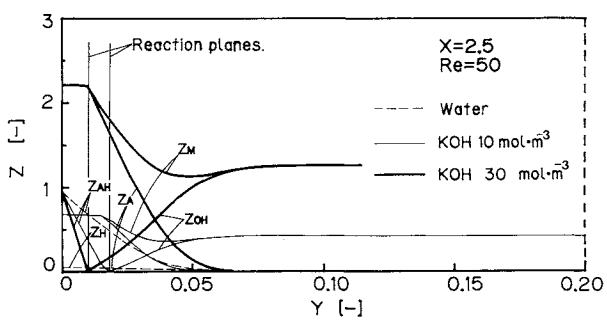

Fig. 9. Theoretical distribution of individual species along the Y direction at $X=2.5$ for dissolution in water, 10 mol·m^{-3} and 30 mol·m^{-3} KOH solution.

the same conditions as in Fig. 8, for water, 10 mol·m^{-3} and 30 mol·m^{-3} KOH solutions. These profiles are steeper and the reaction planes form closer to $Y=0$ than at $X=12.5$. Therefore rates of dissolution are faster near the entrance.

Conclusion

Dissolution of benzoic acid from the wall of a parallel-plate duct into laminar streams of aqueous KOH or LiOH solutions was satisfactorily modeled using diffusion equations which take into account the chemical and ionic interactions between the different species in solution. Theoretical overall rates of dissolution (obtained through finite-difference numerical calculations) were experimentally verified for Reynolds numbers between 50 and 150 and alkali concentrations up to 30 mol·m^{-3}. The numerical technique used in the theoretical analysis proved efficient and provided not only accurate overall rates of dissolution but also local concentration profiles of all species. It was found that due to the larger mobility of the K^+ ions, dissolution in KOH solutions was faster than in LiOH solutions of equal concentration.

Appendix

The overrelaxation factors β_1 and β_5 are calculated as follows. First, the residuals of Eqs. (23) and (24) at node (J, L) are denoted by ERR1 and ERR2, that is,

$$\mathrm{ERR1}=\frac{S_{AH}}{(\Delta Y)^2}\{Z^{(k)}_{AH_{J,L+1}}-2Z^{(k)}_{AH_{J,L}}+Z^{(k)}_{AH_{J,L-1}}\}$$
$$+\frac{S_A}{(\Delta Y)^2}\{Z^{(k)}_{A_{J,L+1}}-2Z^{(k)}_{A_{J,L}}+Z^{(k)}_{A_{J,L-1}}\}$$
$$-\frac{S_A}{\Delta Y}\left\{\frac{Z^{(k)}_{A_{J,L+1}}+Z^{(k)}_{A_{J,L}}}{2}P^{(k)}_{J,L}-\frac{Z^{(k)}_{A_{J,L}}+Z^{(k)}_{A_{J,L-1}}}{2}Q^{(k)}_{J,L}\right\}$$
$$-\frac{V}{\Delta X}\{(Z^{(k)}_{AH_{J,L}}+Z^{(k)}_{A_{J,L}})-(Z_{AH_{J-1,L}}+Z_{A_{J-1,L}})\} \qquad \text{(A-1)}$$

$$\mathrm{ERR2}=\frac{S_M}{(\Delta Y)^2}\{Z^{(k)}_{M_{J,L+1}}-2Z^{(k)}_{M_{J,L}}+Z^{(k)}_{M_{J,L-1}}\}$$
$$+\frac{S_M}{\Delta Y}\left\{\frac{Z^{(k)}_{M_{J,L+1}}+Z^{(k)}_{M_{J,L}}}{2}P^{(k)}_{J,L}-\frac{Z^{(k)}_{M_{J,L}}+Z^{(k)}_{M_{J,L-1}}}{2}Q^{(k)}_{J,L}\right\}$$
$$-\frac{V}{\Delta X}\{(Z^{(k)}_{M_{J,L}}-Z_{M_{J-1,L}})\} \qquad \text{(A-2)}$$

Suppose now that the Z_i's at node (J, L) are corrected so as to make the residuals equal zero. The new Z_i's are defined by

$$Z^{(k+1)}_i=\beta_i\cdot Z^{(k)}_i \qquad \text{(A-3)}$$

where the β_i's are overrelaxation factors to be derived next. By definition, replacement in Eqs. (A-1) and (A-2) of $Z^{(k)}_i$ by $Z^{(k+1)}_i$, i.e., by $\beta_i\cdot Z^{(k)}_i$, reduces ERR1 and ERR2 to zero. This operation leads to the following expressions:

$$\mathrm{ERR1}=(\beta_1-1)\left\{\frac{2S_{AH}}{(\Delta Y)^2}+\frac{V}{\Delta X}\right\}\cdot Z^{(k)}_{AH_{J,L}}$$
$$+(\beta_2-1)\left\{\frac{2S_A}{(\Delta Y)^2}+\frac{S_A}{\Delta Y}\left(\frac{P^{(k)}_{J,L}-Q^{(k)}_{J,L}}{2}\right)+\frac{V}{\Delta X}\right\}\cdot Z^{(k)}_{A_{J,L}} \qquad \text{(A-4)}$$

$$\mathrm{ERR2}=(\beta_5-1)\left\{\frac{2S_M}{(\Delta Y)^2}-\frac{S_M}{\Delta Y}\left(\frac{P^{(k)}_{J,L}-Q^{(k)}_{J,L}}{2}\right)+\frac{V}{\Delta X}\right\}\cdot Z^{(k)}_{M_{J,L}} \qquad \text{(A-5)}$$

β_5 can be solved directly to give

$$\beta_5=1+\frac{\mathrm{ERR2}/Z^{(k)}_{M_{J,L}}}{\dfrac{2S_M}{(\Delta Y)^2}-\dfrac{S_M}{\Delta Y}\left(\dfrac{P^{(k)}_{J,L}-Q^{(k)}_{J,L}}{2}\right)+\dfrac{V}{\Delta X}} \qquad \text{(A-6)}$$

As for β_1, the following relation is first derived from Eq. (A-3):

$$\frac{1-\beta_2}{1-\beta_1}\cdot\frac{Z^{(k)}_{A_{J,L}}}{Z^{(k)}_{AH_{J,L}}}=\frac{Z^{(k+1)}_{A_{J,L}}-Z^{(k)}_{A_{J,L}}}{Z^{(k+1)}_{AH_{J,L}}-Z^{(k)}_{AH_{J,L}}} \qquad \text{(A-7)}$$

The right-hand side of Eq. (A-7) is then approximated to a partial derivative, $\partial Z_A/\partial Z_{AH}$. This derivative can be obtained from Eqs. (12) and (13). The result is

$$G\left(\equiv\frac{1-\beta_2}{1-\beta_1}\cdot\frac{Z^{(k)}_{A_{J,L}}}{Z^{(k)}_{AH_{J,L}}}\right)=\frac{K_1\{(Z^{(k)}_{H_{J,L}})^2+K_2\}}{\{Z^{(k)}_{H_{J,L}}\}^2\cdot\{2Z^{(k)}_{H_{J,L}}+Z^{(k)}_{M_{J,L}}\}} \qquad \text{(A-8)}$$

β_1 is finally obtained by proper manipulation of Eqs. (A-4) and (A-8):

$$\beta_1 = 1 + \frac{\mathrm{ERR1}/Z^{(k)}_{AH_{J,L}}}{\left\{\frac{2S_{AH}}{(\Delta Y)^2} + \frac{V}{\Delta X}\right\} + \left\{\frac{2S_A}{(\Delta Y)^2} + \frac{S_A}{\Delta Y}\left(\frac{P^{(k)}_{J,L} - Q^{(k)}_{J,L}}{2}\right) + \frac{V}{\Delta X}\right\} \cdot G} \tag{A-9}$$

Acknowledgment

The authors would like to thank Mr. Yoshimi Kanno for his assistance in part of the experimental work of this study.

Nomenclature

A^-, AH	=	anionic and molecular benzoic acids	
C	=	concentration	[mol·m^{-3}]
C^*_T	=	solubility of benzoic acid in water	[mol·m^{-3}]
D	=	diffusion coefficient	[m^2·s^{-1}]
ERR1, ERR2	=	residuals defined by Eqs. (A-1) and (A-2)	[—]
F	=	Faraday's constant	[A·s·mol^{-1}]
$\mathscr{F}$	=	integral normal flux of total benzoic acid at $Y=0$	[—]
G	=	factor defined by Eq. (A-8)	[—]
$\vec{i}, \vec{j}$	=	unit vectors along X and Y	[—]
K_{AH}	=	dissociation constant of benzoic acid	[mol·m^{-3}]
K_W	=	ionization product of water	[mol^2·m^{-6}]
K_S	=	solubility constant of molecular benzoic acid in water	[mol·m^{-3}]
K_1	=	dimensionless dissociation constant of benzoic acid, K_{AH}/C^*_T	[—]
K_2	=	dimensionless ionization product of water, K_W/C^{*2}_T	[—]
K_3	=	dimensionless solubility constant of molecular benzoic acid in water, K_S/C^*_T	[—]
l	=	duct's length (see Fig. 4)	[mm]
$\mathscr{M}$	=	dimensionless overall rate of dissolution	[—]
N	=	mass flux	[mol·m^{-2}·s^{-1}]
$\mathscr{N}$	=	dimensionless mass flux, $N/6\bar{v}C^*_T$	[—]
n	=	valence	[—]
P, Q	=	electric potential terms defined by Eqs. (25) and (26)	[—]
R	=	gas constant	[kg·m^2·s^{-2}·K^{-1}·mol^{-1}]
$\mathscr{R}$	=	dimensionless reaction rate $r\delta/6\bar{v}C^*_T$	[—]
r	=	reaction rate	[mol·s^{-1}·m^{-3}]
Re	=	Reynolds number, $\bar{v}\delta/\gamma$	[—]
S	=	dimensionless diffusion coefficient, $D/6\gamma Re$	[—]
Sc	=	Schmidt number, γ/D_{AH}	[—]
T	=	absolute temperature	[K]
V	=	dimensionless velocity, $Y-Y^2$	[—]
$\bar{v}$	=	average velocity inside duct	[m·s^{-1}]
X	=	dimensionless x coordinate, x/δ	[—]
x	=	coordinate parallel to flow	[m]
Y	=	dimensionless y coordinate, y/δ	[—]
y	=	coordinate normal to flow	[m]
Z	=	dimensionless concentration C/C^*_T	[—]
$\bar{Z}_{T_{out}}$	=	mixing cap concentration of total benzoic acid at exit	[—]
$\beta_1, \beta_2, \beta_5$	=	relaxation factors	[—]
Δ	=	delta (difference) operator	
δ	=	duct height (see Fig. 4)	[mm]
γ	=	kinetic viscosity of water	[m^2·s^{-1}]
Φ	=	dimensionless electric potential, $F\phi/RT$	[—]
ϕ	=	electric potential	[kg·m^2·s^{-3}·A^{-1}]

〈Subscripts〉

A^-, AH	=	anionic and molecular benzoic acids
aq	=	aqueous
H, OH, Li, K	=	ions in solution
i	=	species code: $1=AH$, $2=A^-$, $3=OH^-$, $4=H^+$, $5=M^+$
J, L	=	grid point coordinate (see Fig. 2)
JT	=	number of nodes in X direction
LT	=	number of nodes in Y direction
M (=K$^+$, Li$^+$)	=	metal
M_0	=	metal at inlet of testing zone
s	=	solid
T	=	total (molecular+anionic) benzoic acid

〈Superscripts〉

(k)	=	iteration step
*	=	saturated state in pure water
$\rightarrow$	=	vector

Literature Cited

1) Acrivos, A.: *Chem. Eng. Sci.*, **13**, 57 (1960).
2) Bamford, C. H. and C. F. H. Tipper: "Comprehensive Chemical Kinetics," Vol. 8, p. 209, Elsevier, Amsterdam (1977).
3) Bauer, H. F.: *Int. J. Heat Mass Transfer*, **19**, 479 (1976).
4) Eigen, M. and M. Eyring: *J. Am. Chem. Soc.*, **84**, 3254 (1962).
5) Friedlander, S. K. and M. Litt: *Chem. Eng. Sci.*, **7**, 229 (1958).
6) "International Critical Tables," Vol. 6, p. 152, McGraw-Hill, New York (1933).
7) "International Critical Tables," Vol. 6, p. 279, McGraw-Hill, New York (1933).
8) Isenberg, J. and G. de Val Davis: "Topics in Transport Phenomena," C. Gutfinger, ed., p. 482, Hemisphere, Washington (1975).
9) Levich, V. G.: "Physicochemical Hydrodynamics," p. 279, Prentice-Hall, New Jersey (1962).
10) Litt, M. and S. K. Friedlander: *AIChE J.*, **5**, 483 (1959).
11) Newman, J. S.: "Advances in Electrochemistry and Electrochemical Engineering," C. W. Tobias, ed., Vol. 5, p. 107, Wiley Interscience, New York (1967).
12) Nippon Kagaku Kai (ed.): "Kagaku Binran Kiso Hen," Vol. 2, p. 812, Maruzen, Tokyo (1975).
13) Robinson, R. A. and R. H. Stokes: "Electrolyte Solutions," 2nd ed., p. 463, Butterworths Pub., London (1959).
14) Roszak, J. and M. K. Obrebska: *Int. J. Heat Mass Transfer*, **20**, 535 (1977).
15) Sandblom, J.: *J. Phys. Chem.*, **73**, 249 (1969).
16) Shames, I. H.: "Mechanics of Fluids," 2nd ed., p. B-36, McGraw-Hill (1982).
17) Vanadurongwan, V., C. Laguerie and J. P. Coudere: *Can. J. Chem. Eng.*, **54**, 460 (1976).

(Presented at the 49th Annual Meeting of the Society of Chemical Engineers, Japan, at Nagoya, April 3, 1984.)